2020 IEEE/RSJ International Conference on Intelligent Robots and Systems (IROS)
October 25-29, 2020, Las Vegas, NV, USA (Virtual)

Introduction to 7-DoF CoSMo-Arm : High Torque Density Manipulator based on CoSMoA and E-CoSMo

Jaeho Noh, Jaeyong Lee, Seyoung Cheon, and Woosung Yang, *Member, IEEE*

Abstract- **This study proposes a novel 7-DOF robotic manipulator called CoSMo-Arm for high torque density multi-link robotic platform based on a concentrically stacked modular actuator (CoSMoA) and an extended coaxial spherical joint module (E-CoSMo) introduced in previous researches. The CoSMoA is an actuator module designed to improve thermal characteristics by stacking the motor actuator parts to share the heat dissipation device of the adjacent actuator module, thereby theoretically amplifying motor performance by approximately 3.2 times. The E-CoSMo is a parallel joint mechanism connected to the end of the CoSMoA to create point-centered rotational four degrees of freedom. This joint module has a large range of motion in specific rotational directions and maximum output of approximately up to four times to the actuator output in the specific workspace. The CoSMo-Arm is designed to take advantages of these novel concept modules, having a higher payload than its own weight. To verify the benefits of the proposed mechanism, we performed kinematic analysis and dynamics simulations. From experimental verifications of the real prototype, the feasibility and validity are confirmed as a multi-DOF robotic manipulator.**

I. INTRODUCTION

Recently, various studies have attempted to extend the working area of robots to human activity areas, by mounting dexterous manipulators on mobile platforms [1-4]. The mobile platforms extend the workspace and degrees of freedom (DOF) of the robots, enhancing the ability to perform tasks for various applications. The manipulators operated on mobile platforms require high torque density and lightweight [3-4], simultaneously. These high performance requirements for manipulators are one of the reasons to delay the usability expansion of the robots.

There are two typical ways to improve the payload of the system while maintaining the weight of the system. The first method is to improve the mechanical components and structure materials related to driving performance of the system. The second is to enhance the performance by the advancement of mechanism. The representative examples of the component improvement are to use a lightweight, high-rigidity material such as carbon-reinforced fiber to reduce the weight of the system, and to apply a high-performance motor. Particularly in electrically actuated system, in order to achieve high payload per weight ratio, the drive module needs to have high torque density. However, due to physical limitations, the power or torque per weight of the drive module has not been greatly improved lately [5-7]. Therefore, in some robotic systems, the performance of electric motors has improved by adding a forced cooling system to the driving module. In addition, the field weakening control method has been adopted so that power density of the electric actuator improves [5-7].

Second, a special mechanism such as parallel mechanisms is used and this, in general, is optimized for the purpose [5-7]. By adopting this mechanism, the multiple actuator modules, which has relatively large amount of the mass compared to other parts, can be placed on the base frame [5,8,9]. Due to this feature, the driving system inertia is reduced and the design constraint of the actuator module is flexible. Thus, the payload capacity of the system is independent of the mass of the actuator module located at the base frame. Also, the output power of the actuator is summed up within a specific workspace, thereby the power capacity of the drive module becomes increased [5-7]. On the other hand, the operating range of the robot based on the parallel mechanism is smaller than that of the series robot arm. However, in the case of the manipulator with the mobile platform, the decreased range of motion can be compensated by the supplementary mobility.If those two methodologies are adopted simultaneously, the payload per mass of the system can be further enhanced. Inspired from this, we have proposed a special type of actuator modules and a spherical-parallel joint module in the previous studies [5]. In this work, we introduce a 7-DOF robotic arm that utilizes the characteristics of the aforementioned two modules and confirm the feasibility of the proposed system.

In the proposed novel mechanism, the multiple actuator modules were intensively placed on the base frame, reducing the mass of the moving part and concentrating the heat source. The system frees from disturbance torque owing that rotor to rotate in high speed is located at the base part. In addition, a point-centered 4-DOF joint module which combines a spherical parallel mechanism and a universal joint to effectively utilize the output of the drive module is exploited as the shoulder and wrist joints of the proposed robotic arm. The spherical joint module determines the 3-DOF rotation angle, and the universal joint creates 1-DOF rotation additionally. The unique joint mechanism can distribute the output of the actuator modules to multiple axes, thereby the torque output can be amplified up to 3 times in the specific range of motion (ROM) [8].

* This research was supported by the Basic Science Research Program through the National Research Foundation of Korea (NRF) funded by the Ministry of Education (2017R1A2B3010336)

J. Noh, J. Lee, S. Cheon and W. Yang are with the Kwangwoon University, Seoul, Republic of Korea (e-mail: {causeim, leejy93, cheon798 dreamrize}@kw.ac.kr).

The paper is composed as follows; Section II describes the overall features and configuration of the proposed system. The kinematic analysis method and kinematics based position control for verification are introduced in section III. Section IV discuss the simulation and experiment results to verify the feasibility of the proposed system. Section 5 summarizes the results of this work.

II. CoSMo-Arm

In this section, we newly introduce a novel robotic mechanism consists of a concentrically stacked modular actuator (CoSMoA) and an extended coaxial spherical joint module (E-CoSMo). The system incorporating these two modules is called the n-DOF CoSMo robotic system. In special, in this work, a new 7-DOF robotic manipulator based on these modules is proposed as shown in Fig. 1(b). Figure 1(a) represents the joint configuration of a typical serial arm. The 7-DOF CoSMo-Arm has 3-DOF coaxial spherical joint module and the E-CoSMo, which generate 3-DOF wrist rotation, 1-DOF elbow rotation, and 3-DOF shoulder rotation (Fig. 1). The lengths of the upper and lower arms are 325 mm and 348 mm respectively, and the mass of whole system is about 18 kg. We call this system CoSMo-Arm 1.0. Our previous studies have shown that the CoSMoA and E-CoSMo system have maximum 3.2 and 4 times enhanced torque output compared to naturally cooled actuator modules, respectively [5,12]. Thus, in limited circumstances, the proposed system has up to 9.6 times larger power output than a single actuator module. Fig. 2 represents the real CoSMo-Arm based on the design of Fig 1. (b)

A. The CoSMoA

The right side of Fig. 3 (a) and (b) shows the cross section view of the CoSMoA applied to the E-CoSMo and the CoSMo respectively. the CoSMoA applied to the E-CoSMo is driven through Thingap's slotless BLDC motor, LSI-105 (early prototype version), and CSD-type Harmonic Drive with a 100:1 reduction ratio. The module is also includes RLS's AkSiM magnetic encoders for gear input and output. The outside of the housing is equipped with a radiator fin for heat dissipation, as well as an axially-connected air tunnel. With this configuration, the CoSMoA is characterized by simultaneously being cooled through a single air flow source. The radiator fin on the housing is in physical contact with the adjacent module. The temperature of the actuator modules become uneven depending on the heat load applied to them. Here, heat is transferred among the actuator modules, and the distributed heat is cooled through the radiator fins incorporated on the respective housings. In a previous study, we confirmed through experimentation that the maximum continuous current through forced cooling is 3.2 times higher than that of a natural cooling environment [5]. Accounting for the characteristics of a slotless motor relatively free from magnetic saturation [10], assuming that the torque increases linearly with increasing current, the proposed actuator module has a continuous torque of approximately 5.6 Nm in a forced cooling environment. (Table 1)

The CoSMo Actator applied to the wrist joint is directly driven through an actuator module using Kollmorgen's Slotted BLDC Motor and TBM-6025A.(Fig. 3) According to the manufacturer's simulation tool, it has a continuous stall torque of 1.45 Nm, approximately twice that when operated in a suitable cooling environment [11].

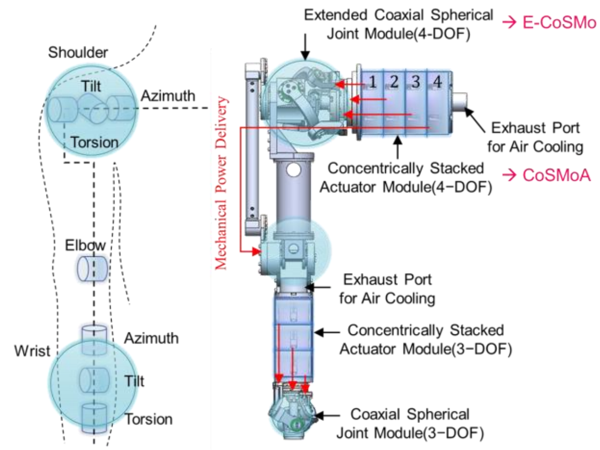

(a) (b)

Figure 1. Joint configuration of serial robot arm (a) compared to the CoSMo-Arm (b)

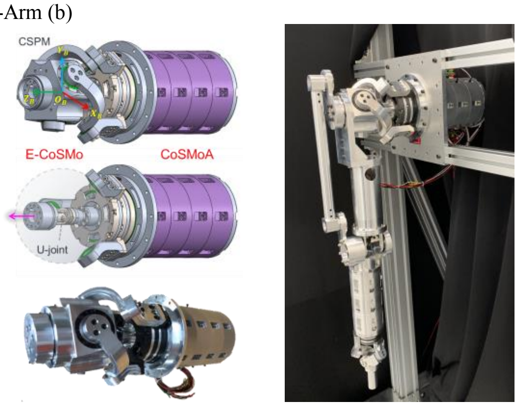

(a) (b)

Figure 2. (a) shows the modular assembly with the E-CoSMo and the CoSMoA [8], and (b) shows the prototype of the proposed CoSMo-Arm.

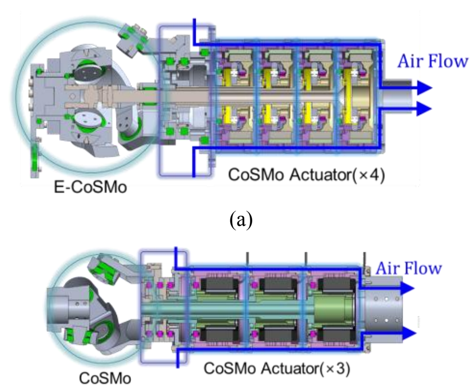

(b)

Figure 3. Cross section views of the 4-DOF CoSMo for the shoulder joint (a) [5,8] and the 3-DOF CoSMo for the wrist joint (b)

TABLE I. A SPECIFICAATION OF MOTOR ADOPTED ON COSMOA

Specification	*LSI-105*	*TBM-6025*	*Unit*
Cont. Stall Torque (Natural Cooling)	1.76	0.727	Nm
Cont. Stall Torque (Forced Cooling)	5.6	1.45	Nm
Cont. Current (Natural Cooling)	6.4	5.6	A
Cont. Current (Forced Cooling)	20	11	A
No Load Speed	4600	2630	rpm
Continuous Power	850	144	W
Diameter	105	60	mm
Stator Length	25.4	34	mm
Mass	0.65	0.398	kg

TABLE II. THE MAXIMUM TORQUE CAPACITY OF COSMO-ARM 1.0

Joint	axis	*Actuator Cap. (Amp. Ratio 9.6)*	*Gear Cap. (Repeated Peak)*	*Unit*
Shoulder	Azimuth	16.9	330	*Nm*
	Tilt	8.5	150	*Nm*
	Torsion	8.5	150	*Nm*
Elbow	Pitch	5.6	110	*Nm*
Wrist	Azimuth	4.35	4.35	*Nm*
	Tilt	2.2	2.2	*Nm*
	Torsion	2.2	2.2	*Nm*

B. The E-CoSMo

The E-CoSMo is a mechanism comprising a coaxial spherical parallel mechanism (CSPM) of 3-DOF and a U-joint (Fig 1). All active drive shafts in the CSPM are coaxially arranged; thus, all joints have 4 rotational DOF for one point. In addition, due to the coaxially configured input rotation axis, the mechanism has a wide ROM with no constraints for a specific axial direction (Table 3). The drive shaft of the extended joint through the U-joints are arranged coaxially with the drive shafts of the CSPM, and its center of rotation is coinciding with the center of the CSPM. The direction of the output shaft of the extended joint is determined by the CSPM and drives an additional 1 degree of freedom for the respective axis.

TABLE III. ROM OF THE E-COSMO AND THE COSMO-ARM 1.0

Joint Location	E-CoSMo		CoSMo-Arm	
	Axis	*RoM (Deg)*	*Corresponding Joint*	*RoM (Deg)*
Shoulder	Azimuth	$\pm\infty$	330	$\pm\infty$
	Tilt	$\pm\mathbf{45}$	150	$\pm\mathbf{30}$
	Torsion	$\pm\infty$	150	$\pm\infty$
Elbow	Pitch	$\pm\infty$	110	**10-170**
Wrist	Azimuth	$\pm\infty$	4.35	$\pm\infty$
	Tilt	$\pm\mathbf{45}$	2.2	$\pm\mathbf{45}$
	Torsion	$\pm\infty$	2.2	$\pm\infty$

The proposed E-CoSMo is applied to the part corresponding to the shoulder-elbow joint of the human body, and was designed so that the 4-DOF CoSMoA, comprising nearly half the weight of the CoSMo-Arm, could be removed from the moving part. Through the parallel mechanism feature, when directional force is applied to a certain axis, the combined action of the actuator allows the force to be distributed. This results in torque output performance of up to approximately three to four times that of an actuator in a specific axial direction in shoulder joint [8, 22]. Considering the rise in output due to forced cooling, the output torque in the pitch axis direction of the shoulder is about 5.6 Nm, and the output torque is about 4.35 Nm in the roll direction of the wrist. For the shoulder joint, considering the output summing effect of the joint module and the torque amplification rate of the reducer, torque can be theoretically output up to 1,690 Nm in the sagittal plane. However, the output was limited considering the stiffness of the output shaft and the torque limit of the reducer.

III. ANALYSIS ON KINEMATICS

In this section, we discuss a method for obtaining the kinematic relationship between the task space and the active joint space of the CoSMo-Arm, through a virtual 7-DOF robot arm joint space. We also discuss a control scheme based on closed-loop inverse kinematics to verify this method. The design parameters are selected from the previous work, which has no singularity on the workspace while guaranty kinematic performance [8].

A. Jacobian of the E-CoSMo

Due to the spherical rotation mechanism, the rotational Jacobian is the only Jacobian of the E-CoSMo. The output angular velocity of the CSPM can be expressed as the vector sum of all revolute joints [8]. The relationship between input and output angular velocity through the universal joint is well known through previous studies. These kinematics are applied in combination to derive the Jacobians of the entire E-CoSMo. Fig. 4 shows a simple schematic of the E-CoSMo. First, if the active drive shaft angle of the spherical parallel structure is θ_1, θ_2, and θ_3 in order, and the active drive shaft angle of the extended degree of freedom is θ_u, then the input state can be composed through $\boldsymbol{\Theta_e} = [\theta_1, \theta_2, \theta_3, \theta_u]^T$. The 3-DOF rotation angles of the output are Z-X-Z Euler rotations; in order, this is shown as Azimuth(q_{az})-tilt(q_{ti})-torsion(q_{to}). The output angle of the extended degree of freedom, which is further rotated with respect to the torsion axis of the output coordinate system of the CSPM, is expressed as μ. The output state of E-CoSMo is expressed as $\boldsymbol{Q_e} = [q_{az}, q_{ti}, q_{to}, \mu]^T$. $\boldsymbol{u_i}$, $\boldsymbol{w_i}$, and $\boldsymbol{v_i}$ indicate the rotation axes of the rotation joints forming the *i*-th link chain of the CSPM, with $i = 1,2,3$. First, using the vector of the CSPM rotation axes, the output angular velocity of the CSPM can be derived as follows [8]:

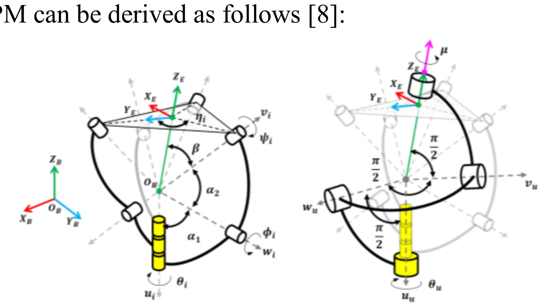

(a) (b)

Figure 4. Joint configuration of the E-CoSMo [8]; (a) represensts the 3-DOF CoSMo and (b) the 4-DOF E-CoSMo. The kinematic scheme is the same even if the u-joint is assembled inside or outside.

$$\boldsymbol{A_a} = [(\boldsymbol{w_1} \times \boldsymbol{v_1})^T \quad (\boldsymbol{w_2} \times \boldsymbol{v_2})^T \quad (\boldsymbol{w_3} \times \boldsymbol{v_3})^T]^T, \qquad (1)$$

$$\boldsymbol{B_a} = diag\left(\begin{bmatrix}(\boldsymbol{w_1} \times \boldsymbol{v_1}) \cdot \boldsymbol{u_1} \\ (\boldsymbol{w_2} \times \boldsymbol{v_2}) \cdot \boldsymbol{u_2} \\ (\boldsymbol{w_3} \times \boldsymbol{v_3}) \cdot \boldsymbol{u_3}\end{bmatrix}\right), \tag{2}$$

$$\boldsymbol{T_a} = \begin{bmatrix}\cos(q_{ti})\cos(q_{az}) & -\sin(q_{az}) & 0 \\ \cos(q_{ti})\sin(q_{az}) & \cos(q_{az}) & 0 \\ -\sin(q_{ti}) & 0 & 1\end{bmatrix}, \tag{3}$$

$$\dot{\boldsymbol{Q}}_{\boldsymbol{a}} = (\boldsymbol{A_a}\boldsymbol{T_a})^{-1}\boldsymbol{B_a}\dot{\boldsymbol{\Theta}}_{\boldsymbol{a}}, \tag{4}$$

where, $\boldsymbol{Q_a} = [q_{az}, q_{ti}, q_{to}]^T$, $\boldsymbol{\Theta_a} = [\theta_1, \theta_2, \theta_3]^T$, and $\boldsymbol{T_a}$ is analytical Jacobian that transform the axial angular velocity to Euler rotation angular velocity. Through this, $\boldsymbol{J_a} = (\boldsymbol{A_a}\boldsymbol{T_a})^{-1}\boldsymbol{B_a}$ is derived.

Next, let the input and output shaft angle of the universal joint is α_3, then the input-output kinematic relationship is derived as $\cos\alpha_3 \tan\mu = \tan\theta_u$. α_3 is defined by the rotation of the CSPM. This can be summarized as follows:

$$\dot{\mu} = \left(\frac{d}{d\theta_u}\operatorname{atan}\left(\frac{\tan(\theta_u)}{\cos(\alpha_3)}\right)\right)\dot{\theta}_u. \tag{5}$$

We can therefore derive the Jacobian $J_u = \frac{d}{d\theta_u}\operatorname{atan}\left(\frac{\tan(\theta_u)}{\cos(\alpha_3)}\right)$ of the universal joint.

Accordingly, by combining (4) and (5), the relationship between $\dot{\boldsymbol{Q}}_{\boldsymbol{e}}$ and $\dot{\boldsymbol{\Theta}}_{\boldsymbol{e}}$ can be derived as follows :

$$\dot{\boldsymbol{Q}}_{\boldsymbol{e}} = \begin{bmatrix}\boldsymbol{J_a} & \boldsymbol{0_{3\times1}} \\ \boldsymbol{0_{1\times3}} & J_u\end{bmatrix}\dot{\boldsymbol{\Theta}}_{\boldsymbol{e}}. \tag{6}$$

From this, the Jacobian of the E-CoSMo is derived as $\boldsymbol{J_e} = \begin{bmatrix}\boldsymbol{J_a} & \boldsymbol{0_{3\times1}} \\ \boldsymbol{0_{1\times3}} & J_u\end{bmatrix}$.

B. Virtual kinematics

First, let the position and Euler angles in task space are $\boldsymbol{P} \in \mathfrak{R}^{3\times1}$ and $\boldsymbol{\Omega} \in \mathfrak{R}^{3\times1}$, respectively. then the state of the end effector is expressed as $\boldsymbol{X} = [\boldsymbol{P^T}\ \ \boldsymbol{\Omega^T}]^T$. Next, let the virtual 7-DOF serial-type robot arm is composed of 3-DOF shoulder joints θ_{s1}, θ_{s2}, and θ_{s3} with Z-X-Z Euler rotation, a 1-DOF elbow joint, and θ_{s5}, θ_{s6}, and θ_{s7} as the Z-X-Z Euler rotation 3-DOF wrist joint with respect to the local reference frame $\boldsymbol{R_L}$ on the forearm. The angle state of each joint of the virtual 7-DOF serial robot arm can be expressed as $\boldsymbol{\Theta_s} = [\theta_{s1}, \theta_{s2}, \theta_{s3}, \theta_{s4}, \theta_{s5}, \theta_{s6}, \theta_{s7}]^T$. Let the Jacobian derived from the general serial link analysis as $\boldsymbol{J_s}$, then $\boldsymbol{J_s}$ is expressed as $\left[\dot{\boldsymbol{P}}^{\boldsymbol{T}}\ \ \boldsymbol{\omega}\right]^T = \boldsymbol{J_s}\dot{\boldsymbol{\Theta}}_{\boldsymbol{s}}$ where $\boldsymbol{\omega}$ is a angular velocity of the end effector. Let the analytical Jacobian for the Z-X-Z Euler angle is $\boldsymbol{T_\Omega}$ and $\boldsymbol{T} = \left[\boldsymbol{I_{3\times3}}\ \ \boldsymbol{T_\Omega^{-1}}\right]$, then the velocity state of the task space and the joint space of the virtual serial-type robot arm can be expressed as $\dot{\boldsymbol{X}} = \boldsymbol{T}\boldsymbol{J_s}\dot{\boldsymbol{\Theta}}_{\boldsymbol{s}}$.

Now, the angle of the shoudler and elbow joint of the virtual 7-DoF serial robotic arm can be modeled through the output state of the E-CoSMo. Therefore, $\boldsymbol{Q_e} = [\theta_{s1}, \theta_{s2}, \theta_{s3}, \theta_{s4}]^T$. The 3-DOF wrist joint can also be modeled through the virtual serial link with a base frame of the local reference frame $\boldsymbol{R_L}$ of the robot forearm. Let the input state of the wrist as $\boldsymbol{\Theta_w} = [\theta_5, \theta_6, \theta_7]^T$ and the output state as $\boldsymbol{Q_w} = [\theta_{s5}, \theta_{s6}, \theta_{s7}]^T$, then as shown above, the Jacobian of the wrist is derived based on the CSPM kinematics as $\dot{\boldsymbol{Q}}_{\boldsymbol{w}} = \boldsymbol{J_w}\dot{\boldsymbol{\Theta}}_{\boldsymbol{w}}$.

Let the overall state of the active joints is $\dot{\boldsymbol{\Theta}} = \left[\dot{\boldsymbol{\Theta}}_{\boldsymbol{e}}\ \ \dot{\boldsymbol{\Theta}}_{\boldsymbol{w}}\right]^T$, then the angular velocity relationship between the active joint space and task space become $\dot{\boldsymbol{\Theta}}_{\boldsymbol{s}} = \left[\dot{\boldsymbol{Q}}_{\boldsymbol{e}}\ \ \dot{\boldsymbol{Q}}_{\boldsymbol{w}}\right]^T$, through (6).

$$\dot{\boldsymbol{X}} = \boldsymbol{T}\boldsymbol{J_s}\begin{bmatrix}\boldsymbol{J_e} & \boldsymbol{0_{3\times3}} \\ \boldsymbol{0_{3\times3}} & \boldsymbol{J_w}\end{bmatrix}\dot{\boldsymbol{\Theta}},\ \boldsymbol{J} \in \mathfrak{R}^{6\times7}. \tag{7}$$

This leads to an overall Jacobian of $\boldsymbol{J} = \boldsymbol{T}\boldsymbol{J_s}\begin{bmatrix}\boldsymbol{J_e} & \boldsymbol{0_{3\times3}} \\ \boldsymbol{0_{3\times3}} & \boldsymbol{J_w}\end{bmatrix}$.

C. Analysis with closed-loop inverse kinematics

To verify the kinematics derived above, we perform closed loop inverse kinematics(CLIK) based position control. CLIK is one of the most widely-used methods for obtaining inverse kinematics solutions in robot systems with redundancy. It is an approach using a numerical method. (7) derived above can be expressed as follows for the desired state $\boldsymbol{X_d}$.

$$\boldsymbol{J}(\boldsymbol{\Theta_c})^{+}\dot{\boldsymbol{X}}_{\boldsymbol{d}} = \dot{\boldsymbol{\Theta}}_{\boldsymbol{d}},\ \boldsymbol{J}^{+} \in \mathfrak{R}^{6\times6}, \tag{8}$$

where $\boldsymbol{J}(\boldsymbol{\Theta_c})^{+}$ is the $\boldsymbol{J}(\boldsymbol{\Theta_c})$ pseudo inverse. The subscript *d* and *c* represent the desired and current, respectively. Here, $\dot{\boldsymbol{X}}_{\boldsymbol{d}}$ can be modeled and applied as an first-order feedback control target between current state $\boldsymbol{X_c}$ and desired state $\boldsymbol{X_d}$.

$$\boldsymbol{J}(\boldsymbol{\Theta_c})^{+}\boldsymbol{k_p}(\boldsymbol{X_d} - \boldsymbol{X_c}) = \dot{\boldsymbol{\Theta}}_{\boldsymbol{d}}, \tag{9}$$

where $\boldsymbol{k_p} \in \mathfrak{R}^{6\times6}$ is the gain matrix. By applying $\dot{\boldsymbol{\Theta}}_{\boldsymbol{d}}$ as the desired angular velocity of the active joints of the CoSMo-Arm, it is able to control the end-effector in task space. A simple scheme for control is shown in Fig. 5.

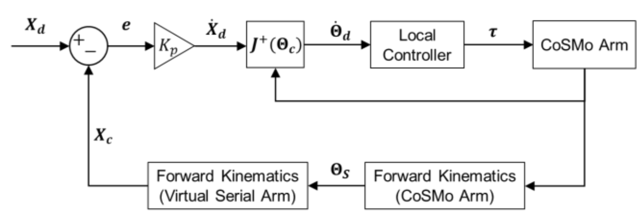

Figure 5. A closed loop inverse kinematics (CLIK) based control scheme.

IV. Verification and Discussion

In this section, we verify the kinematic analysis and dynamic performance of the CoSMo-Arm 1.0 shown in Fig. 1. Then the feasibility of the mechanism is experimentally verified and discussed with the unsolved issues and future work.

A. Kinematics Verification

This simulation was conducted to confirm the end position tracking performance of the 7-DOF manipulator consisting of the CoSMoA and E-CoSMo. The simulation was performed in the Matlab Simmechanics environment, and end trajectory and actuator load were monitored during trajectory control. Fig. 6 (a) shows a snapshot of the CoSMo-Arm during the simulation tracking the target trajectory. The simulation result shows the trajectory tracking performance for two different target trajectories. Through the result of Fig. 6(b), it is confirmed that the control error of the robot end is bounded within 3 mm or less. Hence, we verified the validity of the kinematic analysis and a control algorithm described in previous section. Fig. 7 shows the reachable space of the CoSMo-Arm 1.0 based on kinematic analysis.

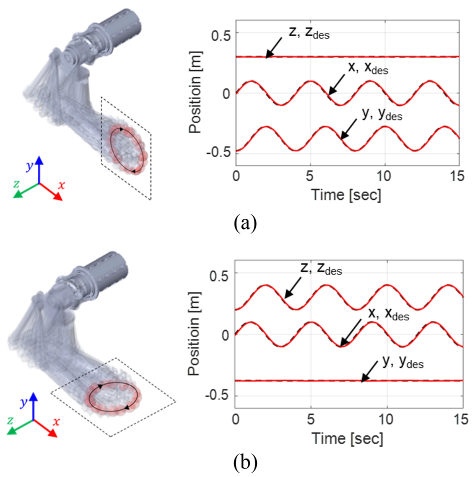

Figure 6. Target trajectory tracking simulation; circular trajectory on sagittal plane (a) and transverse plane (b)

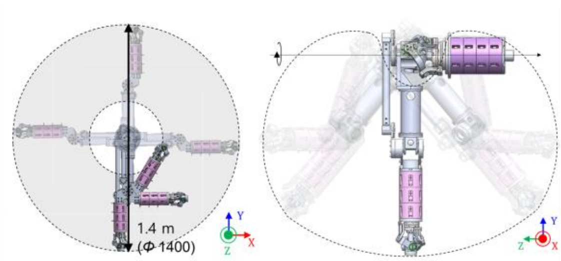

Figure 7. The maximum ROM of the CoSMo-Arm

B. Verification on Torque Amplification Effect

In subsection, one of the performances of the proposed robotic arm is verified in dynamics simulation comparing with an equivalent serial arm designed virtually. Fig. 8(a) shows a lifting motion under a payload of 40 kg. In Fig. 8(b), the consumed currents were calculated theoretically considering the torque constant and gear ratio. The black and red lines represent the currents applied to the CoSMoA and the actuators of the serial arm (see Fig. 1(a)), which has identical center of mass and link length, respectively.

Fig. 9 exhibits the thermal response of motors estimated considering the measured steady-state current [5]. This simulation results were acquired under the same environment condition with thermal parameters of previous work. Comparing Fig. 9(a) with (b), it can be confirmed that the maximum temperature decreases in the forced cooling condition as seen in Fig. 9(b). This means that the forced cooling condition causes to enhancing the maximum load capacity of motors. From Fig. 9(a), it is observed that the proposed mechanism is superior to the general serial arm mechanism in thermal characteristics. In Fig. 9(a), the current applied to the Elb joint is identical with that of the CoSMo_4. However, the Elb one quickly reaches to the limit temperature by comparison with the other in the air-cooling condition. This is because that the proposed CoSMoA mechanism shares the heatsink.

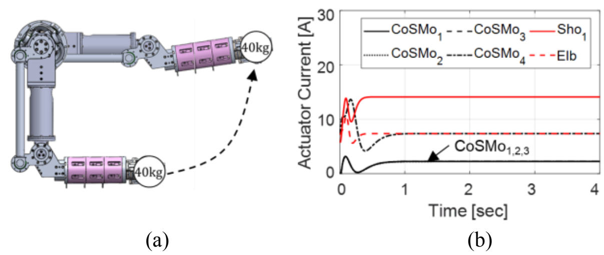

Figure 8. The comparison of the currents applied to each actuator while the arm lifts a 40 kg mass; (a) Snapshots of initial and finished posture; (b) The current plots drawn by the motor in lifting motion

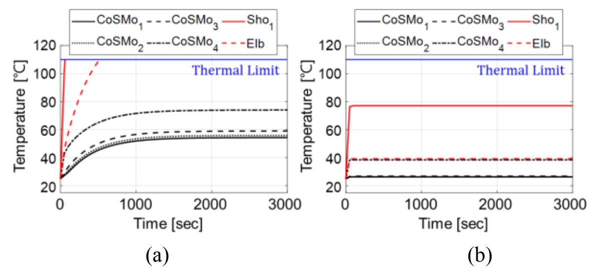

Figure 9. Thermal response of the CoSMoA in the air-cooling condition (a) and forced cooling condition (b) while lifting motion of Fig 7.

In addition, comparing the load currents of Fig. 8(b) and Fig. 9, it is verified that the proposed arm composed of the CoSMoA is operated with lower current than the virtual serial arm irrespective of the cooling effect. This is reason that the E-CoSMo mechanism enables a load torque to be uniformly distributed in the specific ROM and motion. In conclusion, various simulations and verifications give the validity of the proposed robotic arm in enhancing the specific ROM and load capacity.

C. Experimental Verification and Discussion

To verify the feasibility of the CoSMo-Arm, two experimental verifications were performed. The prototype system is controlled in real time at 1 kHz through BECKHOFF's TwinCAT 3 and powered by Elmo's motor driver G-WHI 20/100. First, various experiments of trajectory tracking control were carried out. Fig. 10 shows the snapshots of the circular trajectory tracking corresponding to the dynamics simulation of Fig. 5. It was demonstrated that the robotic arm follows the target trajectory well.

Torque amplification by distributing a load is one of main contributions of the proposed mechanism. Hence, static payload handling test on sagittal plane was conducted. Since the torque and current are proportional, torque amplification can be estimated through the comparison of the active currents applied to the actuators. Fig. 11(a) and (b) show the configuration of the CoSMo-Arm and shows the measured active currents of the shoulder-elbow actuators, respectively. During the test, the shoulder and elbow pitch joints are controlled to keep the position angles at 80 degree and 100 degree under the payload 10 kg, respectively. In Fig. 11(b), the red lines represent the currents measured from the SPM actuators, and the black line represents the current of the universal joint actuator. Due to the mechanical characteristics, the actuators of the SPM and universal joint act on the shoulder pitch simultaneously. Therefore, the shoulder pitch torque is expressed as a sum of the four actuator torques [12]. Blue line indicates the sum of the four actuator currents.

From simulation using the equivalent serial robot model having the mass and motor constant corresponding to the prototype, the shoulder-to-elbow joint current ratio was 2.024. In the related experiment, sum of the four actuator torques to elbow joint torque ratio was calculated as 2.291. This similar result means that the experimental is valid and the torque for the shoulder joint is distributed to the E-CoSMo. The small discrepancy results from differences in dynamics properties such as friction, mass property error, etc. Next, it is noted that the currents to the SPM actuators have similar values each other. This indicates that the torque load applied to the SPM is distributed to the 3-actuators. In particular, it is confirmed that the torque is symmetrically distributed for sagittal motion in which all actuators are simultaneously driven.

Considering the torque capacity of the gear and motor, the CoSMo-Arm shoulder joints theoretically have a continuous torque of 330 Nm or more and speed up to 270 deg/s in the sagittal plane. However, to improve the maximum torque performance of the proposed system, there are unsolved issues remained such as 1) lowering the required motor torque while maintaining torque density, 2) redesigning transmission shaft to have higher rigidity, and 3) revising the gear to have higher torque capacity. Also, since the gear ratio has trade-off with speed characteristics, it should be carefully considered for the required dynamic performance.

V. Conclusion

In this paper, the novel 7-DOF robotic arm was proposed with a unique joint mechanism and actuator module for high torque density multi-link robotic platform. To show the priority of the proposed mechanism, a theoretical kinematic analysis was performed. Various dynamics simulations give the possibility and feasibility as an alternatives of a redundant robot manipulator. In experiments, it is confirmed that the proposed robotic arm mechanism maximizes torque capacity within a limited workspace by improving thermal characteristics and the utilizing the load torque distribution effect of the parallel mechanism. In addition, by placing four actuators on the base, the mass of the moving parts is reduced. Consequently, these characteristics allow the system to support higher payloads than an equivalent serial robot.

In further study, we will analyze the thermal response of the system under various conditions and propose the advanced design maximizing the dynamic performances with extend theoretical analysis. Also, the design will be improved and evaluated considering the rigidity and dynamic properties of the mechanism.

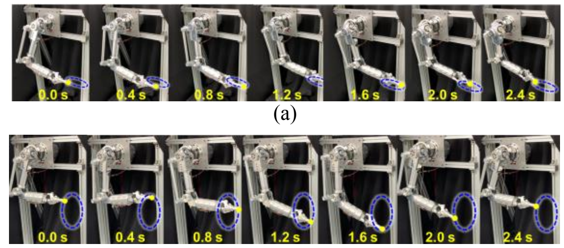

(b)

Figure 10. Experiment snapshot while tracking circular trajectory on transverse plane (a) and sagittal plane (b).

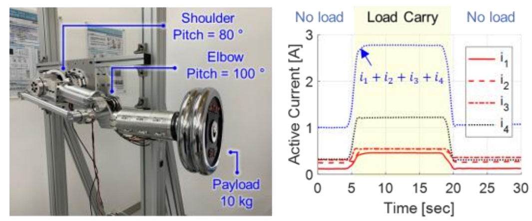

(a) (b)

Figure 11. (a) Configuration of the CoSMo-Arm for the static load test and (b) the currents applied to the shoulder-elbow actuators while handling the 10 kg payload.

References

[1] C. Borst et al., "Rollin' justin-mobile platform with variable base." IEEE Int. Conf. on Robotics and Automation. (ICRA). p. 1597-1598, 2009.
[2] T. Asfour et al., "ARMAR-6: A Collaborative Humanoid Robot for Industrial Environments." IEEE-RAS 18th Int. Conference on Humanoid Robots (Humanoids), p. 447-454, 2018.
[3] E, Johannes, et al. "Overview of the torque-controlled humanoid robot TORO." IEEE-RAS International Conference on Humanoid Robots. IEEE, p. 916-923, 2014.
[4] Kaneko, Kenji, et al. "Humanoid Robot HRP-5P: an Electrically Actuated Humanoid Robot with High Power and Wide Range Joints." IEEE Robotics and Automation Letters, 2019.
[5] Noh, Jaeho, et al. "Design of a Concentrically Stacked Modular Actuator with Forced Air Cooling for Multi-DOF Robotic Systems." Energies vol.11, no. 11, pp 1-13, 2018.
[6] N. Paine and L. Sentis, "Design and Comparative Analysis of a Retrofitted Liquid Cooling System for High-Power Actuators," Actuators, vol. 4, no. 3, pp. 182–202, 2015.
[7] J. Urata, Y. Nakanishi, K. Okada, and M. Inaba, "Design of high torque and high speed leg module for high power humanoid," IEEE/RSJ 2010 Int. Conf. Int. Robot. Syst. (IROS), vol. 28, no. 7, pp. 4497–4502, 2010.
[8] J, Lee, et al. "A Novel Design of Extended Coaxial Spherical Joint Module for a New Modular Type-Multiple DOFs Robotic Platform." IEEE/RSJ Int. Robot. Sys. (IROS), pp 955 – 960, 2018.
[9] R, Brian. "The harmonious robot." Industrial Robot: An International Journal, vol. 33, no. 2, pp. 125-130, 2006.
[10] Permanent magnet DC motor with coreless winding; Technical report; Maxon Motor: Obwalden, Switzerland, 2012.
[11] Kollmorgen, Performance curve design tool, Available online: http://curvegen.kollmorgen.com/, accessed on 1 Mar. 2019.
[12] J. Lee, J. Noh,, S. Lee and W. Yang, "A Novel 4-DoF Robotic Mechanism with E-CoSMo : Kinematics Based Torque Analysis," In 2019 IEEE/RSJ International Conference on Intelligent Robots and Systems (IROS), IEEE.